# Characterization of the operation of RITs with iodine

**IEPC-2017-368**

*Presented at the 35th International Electric Propulsion Conference*
*Georgia Institute of Technology – Atlanta, Georgia – USA*
*October 8–12, 2017*

Waldemar Gärtner*
*Justus Liebig University, Giessen, 35392, Germany*

Daniel Zschätzsch†
*FH Aachen University of Applied Sciences, Aachen, 52064, Germany*

*and*

Kristof Holste‡ Peter J. Klar§
*Justus Liebig University, Giessen, 35392, Germany*

**Abstract: We studied and compared the performance of a RIT 10 operated with iodine and xenon, respectively. In particular, in the case of iodine operation, the performance mapping was accompanied by emission spectroscopic measurements of the plasma inside the discharge chamber. The intensity variations in the emission spectra are indicative for the amounts of the different iodine species in the plasma.**

*Research Assistant, Institute of Experimental Physics I, Waldemar.Gaertner@exp1.physik.uni-giessen.de.
†Student, Faculty of Aerospace Engineering, daniel.zschaetzsch@alumni.fh-aachen.de.
‡senior scientist, Institute of Experimental Physics I,Kristof.Holste@exp1.physik.uni-giessen.de.
§Professor, Institute of Experimental Physics I, peter.j.klar@exp1.physik.uni-giessen.de.

# I. Introduction

At present, the noble gas xenon is mainly used as a propellant for electric propulsion due to its high atomic mass, comparatively low ionization potential, and high collision cross-section. Xenon is rather rare and used in a variety of applications, hence it is getting more and more expensive. An alternative is required and a very promising candidate is iodine[1,2]. Atomic iodine possesses somewhat similar properties in terms of atomic mass and ionization potential than xenon. However, there also are some distinct differences. First, in the gas phase, iodine is present as diatomic molecule. Thus, additional energy for fragmentation needs to be provided during thruster operation in order to generate iodine ions for extraction. Consequently, several different iodine-related species may be present in the discharge chamber of the thruster depending on the operation conditions. Second, a distinct advantage of iodine as propellant is that it is solid at standard conditions, thus, a high pressure storage system is not required which may lead to a significant reduction of weight and costs. Third, iodine is far more chemically reactive than xenon. Therefore, materials issues may become of importance.

# II. Experimental Setup

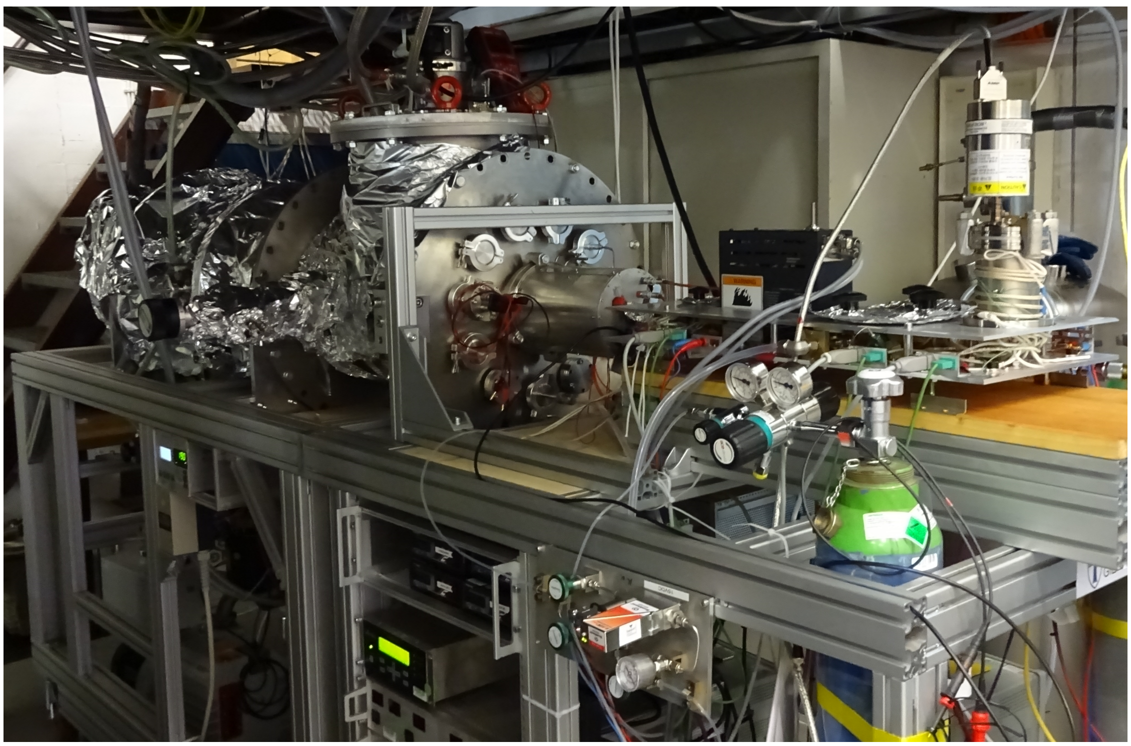

Figure 1: Test setup used for the characterization of RITs, which are operating with iodine.

In order to investigate RITs, which are operated with iodine, a new test setup was built. The setup is shown in Fig. 1. The vacuum chamber has a length of 1.6 m and a diameter of 0.4 m.

## A. Pumping System

The pumping system of the test facility consists of a roughing pump, turbomolecular pump, and a cryogenic pump. Both, the roughing pump and the turbomolecular pump are resistant to corrosive gases. The cryogenic pump consists of a vertical cylindrical trap with five additional ring-like horizontal surfaces, which are evenly distributed along the length of the trap. With the help of a continuous flow of liquid nitrogen, the cryogenic pump achieves a temperature of 80 K, which is sufficient to efficiently freeze out iodine on its surface. The pumping speed of the overall system is about 24000 $\text{ls}^{1}$.

### B. Mass Flow Contol System

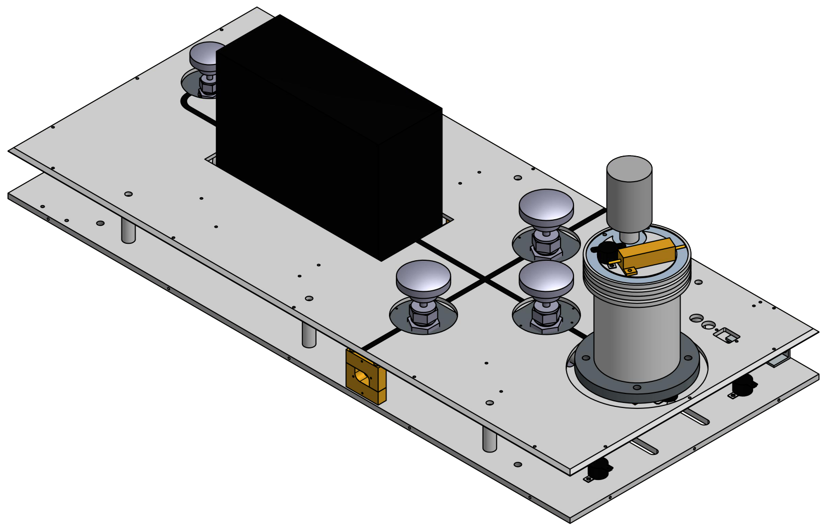

Figure 2: Used mass flow control unit for control the iodine mass flow.

The test setup has two independently operating flow control units. One flow control unit regulates the flow of xenon and the other is used to control the iodine flow. For xenon a calibrated Bronkhorst mass flow controller is used, which can provide a maximum flow of 10 sccm. The mass flow control system built to regulate the iodine flow is shown in Fig. 2. It consists of a reservoir, a pressure gauge, a mass flow controller, supply tubes, and various valves. The iodine reservoir is heated up to 100 °C and possesses, at this temperature, an internal pressure of 30 mbar. We use a Baratron 613B, which operates at a temperature of 150 °C, to measure the pressure of the reservoir. In this way, the resublimation of iodine in the interior of the pressure gauge is avoided. A MKS 1152C is used as mass flow controller for iodine. This controller is specially designed for iodine and can provide an iodine mass flow of up to 20 sccm. Both, the MKS 1152C and the other components of the mass flow control unit are kept at a temperature of 135 °C when operating with iodine. The valves separate three different gas lines within the mass flow control unit. One to the thruster, a second line to the flush gas for the mass flow unit, and a third line to the vacuum chamber. The entire supply system is covered by two metal plates, which are heated up to 100 °C. This avoids temperature fluctuations in the interior of the iodine flow system.

### C. Thruster

For our investigations with iodine as propellant, we used a RIT 10 with a three-grid system with 243 extraction channels. The thickness of the grids and the spacing between the grids are both 1 mm. The holes within the grid system have diameters of 4 mm, 3 mm, and 4 mm, respectively, in ascending order from the plasma to the space environment.

We have used a laboratory radio-frequency generator from APCON for the operation of the thruster. The operation frequency of this generator can be chosen between 1.1 MHz and 3.2 MHz. Furthermore, it can provide an RF-power up to 120 W.

## III. Measurements and Results

### A. Performance Mapping

All measurements have been performed with 1500 V screen-grid voltage and -150 V acceleration-grid voltage. The extracted ion-beam current was defined as the current extracted directly from the plasma minus the current flowing through the acceleration grid. During all measurements a tungsten filament provided electrons for beam neutralization.

The performance curves for xenon and iodine at 1.1 MHz for a preset ion-beam current of 80 mA are directly compared in Fig. 3. The behavior of the two performance curves is typical for the two propellants,

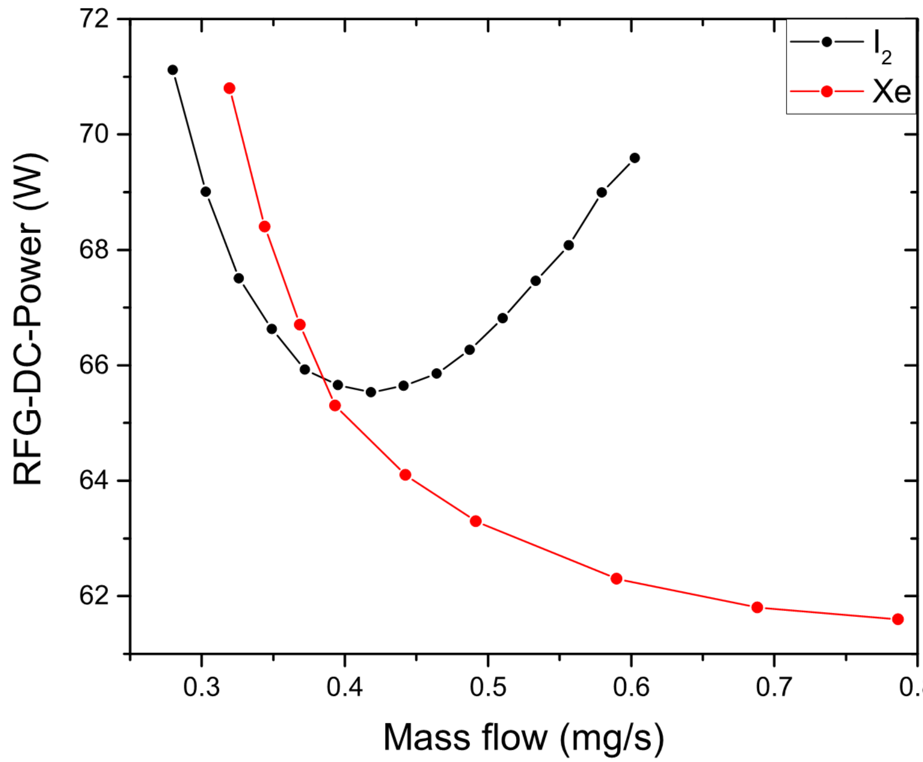


Figure 3: Comparison of the performance mapping of a RIT 10 for xenon and iodine at an ion beam current of 80 mA and an operation frequency of 1.1 MHz of the radio-frequency generator.

similar results have been obtained at different beam currents and for different operating frequencies between 1.1 and 2.2 MHz. At low mass flows, the performance of the RIT-10 with iodine as propellant is better than with xenon. At high mass flows, the situation is inverted, i. e. the performance of the RIT-10 with xenon is better than with iodine. The crossover point where both propellants show the same performance occurs at a mass flow of 0.41 mg/s for this preset value of the ion-beam current. This mass-flow value is just below the mass-flow value corresponding to the optimum performance of the iodine-fueled thruster. It needs to be pointed out that, in case of the xenon-fueled RIT, the optimum performance occurs at a much higher mass flow, in a range just above the highest mass flow studied in this work. It should also be noted that xenon requires a much lower minimal RFG power for keeping up the preset current than iodine. The results are in accordance with the model of Grondein et al[3]. The model predicts a higher efficiency of iodine for propellant mass flow rates, which are below a certain value, depending on the special design of the thruster. The much higher RF power required for keeping up the preset current in case of iodine compared to xenon is striking and indicates that operating the thruster with iodine in this range of mass flows is inefficient. This significantly larger power consumption of the iodine-fueled thruster at high mass flows is very likely related to the molecular nature of iodine. Analyzing the rates of the various reaction channels in Ref. 3 indicates that at higher mass flows, which correspond to lower electron temperatures even at constant ion-beam current (see also Ref. 4), all possible ionization rates decrease and a simultaneous increase of the dissociation rate occurs. Hence, the neutral density increases, which evokes collisional cooling of the electrons and reduces the ionization efficiency further. A closer look at the microscopic plasma properties is required to clarify this behavior.

### B. Optical emission spectroscopy

To obtain a deeper understanding of the physical processes which cause this dramatic increase of the RF-power needed in operating the thruster at high mass flows, we have conducted optical emission spectroscopic studies. These measurements of optical emission spectra from the iodine plasma have been performed with a fiber coupled spectrometer covering the spectral range from 300 to 900 nm with a resolution of 0.26 nm. A condenser lens on a fiber was placed next to the transparent discharge vessel in order to collect the emitted light which was then guided into the spectrometer. The response function of the spectrometer has been determined by measuring the continuous spectrum of a calibrated tungsten lamp. All spectra shown in the following are corrected for the spectral response of the detection system.

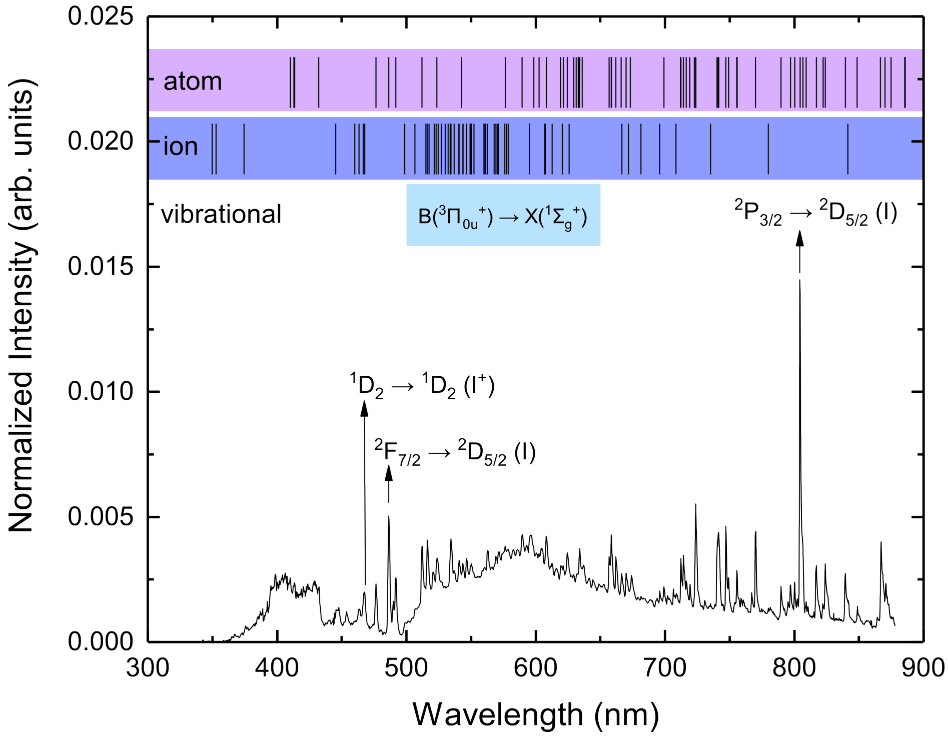


Figure 4: (color online) Optical emission spectrum of the iodine plasma at a mass flow of 0.42 mg/s (1.1 MHz, 80 mA ion beam current). Possible optical transitions of I and $I^+$ taken from the NIST database are shown. The region of the vibrational transitions is indicated.

Fig. 4 shows as an example the optical emission spectrum at ion beam current of 80 mA and an iodine mass flow of 0.41 mg/s. Similar spectra were recorded at each operational point of the performance mapping for iodine shown in Fig. 3. The iodine plasma of the thruster will mainly consist of molecular ($I_2$), atomic (I), and ionized ($I_2^+$, $I^+$) species. All species may exist in the ground or in an excited state[5]. Vibrational excitation can be caused by collisions of electrons with $I_2$ or by collision processes of the type $I^+ + I_2$ or $I_2^+ + I_2$. Negative ions may be produced by dissociative attachment ($e^- + I_2 \rightarrow I^- + I$), but according to Ref. 3 the reaction rate of this process is rather low and may be neglected. The atomic and ionic features of the emission spectrum are sharp lines whereas the vibrational contribution to the spectrum consists of a broad feature between 500 nm and 650 nm. The position of the three wavelength used for a first analysis are indicated (see also Table 1). Due to the absence of atomic and ionic transitions between 640 nm and 650 nm on the broad vibrational background, the integrated intensity of this part of the spectrum was chosen as a measure of the vibrational contribution to the spectrum.

Table 1: List of atomic, ionic, and vibrational transitions of iodine in the optical emission spectra, which have been selected a more essential analysis. Transitions wavelengths $\lambda$ are taken from the NIST database.

| Label | Type | Transition | Wavelength $\lambda$ [nm] (NIST) |
|---|---|---|---|
| atom (1) | I I ($I^0$) | $5p^4 6p\ ^2P_{3/2} \rightarrow 5p^4 6s\ ^2D_{5/2}$ | 804.374 |
| atom (2) | I I ($I_0$) | $5p^4 7p\ ^2F_{7/2} \rightarrow 5p^4 6s\ ^2D_{5/2}$ | 486.232 |
| ion | I II ($I^+$) | $5p^3 6p\ ^1D_2 \rightarrow 5p^3 6s\ ^1D_2$ | 467.553 |
| vibrational | | | 640-650 |

All emission spectra recorded show the same characteristic spectral features, however, the intensities

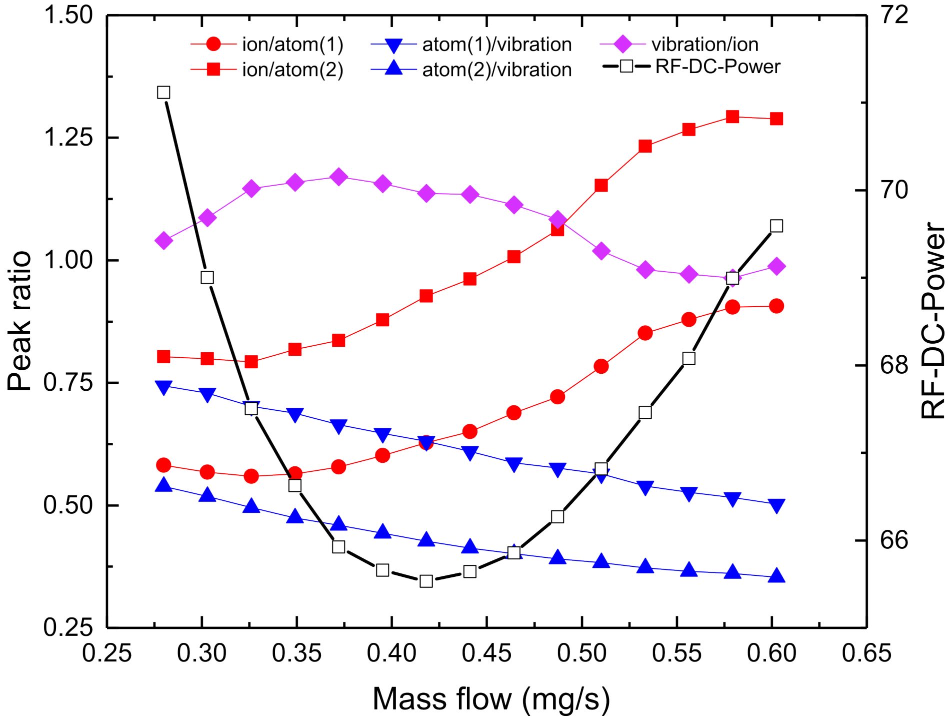


Figure 5: Intensity ratios of the different atomic, ionic, and vibrational transitions together with the corresponding performance curve at 80 mA (from Fig. 3).

vary. This means that atomic $I^0$ and ionic $I^+$ are present in the plasma at all mass flows studied. The same holds for the presence of $I_2$ indicated by the vibrational background. Unfortunately, no conclusions can be drawn about the ionized molecule $I_2^+$ or the doubly ionized $I_2^+$ as the wavelengths of the corresponding spectral features are outside the spectral range under study. Furthermore, as we do not have access to the transition matrix elements of the optical emission processes between the electronic states of the species, we cannot translate the intensities of the spectral features directly to the concentrations of these species inside the plasma. Nevertheless, the variation of the intensity ratio of signals distinct for two species should yield information about the variation of their concentrations with respect to each other. To confirm this, we plot intensity ratios of characteristic features indicated in Fig. 4 and listed in Table 1 as a function of mass flow. Two clear trends can be observed. First, the ion/atom ratio, i.e. $I^+$ to $I^0$, (red curves) increases, but tends to saturate at high mass flows. Second, the atom/ vibration ratio, i.e. $I^0$ to $I_2$, (blue curves) decreases with increasing mass flow. The vibration/ion ratio, i. e. $I_2$ to $I^+$ only varies by about 10% about its mean value, however, seems to exhibit comparatively large values at the minimum of the performance mapping. Our findings seem to indicate that our measurements are performed in a different regime than those discussed in the model calculations of Grondein et al. Our findings for the relative trends of the densities of $I^+$ ions, and $I^0$ atoms, and $I_2$ molecules cannot directly be related to the performance mapping at this point. In particular, they do not yield an explanation of the sharp rise of RF power required to achieve the preset ion beam current at higher mass flows in case of iodine compared to xenon. However, the variation of the density of the molecular species with respect to the atomic species is a clear indication that the neutral gas density during a performance mapping is not simply proportional to the mass flow.

## IV. Conclusion

We have demonstrated that a RIT-10 thruster can be operated with iodine as well as with xenon. The performance with both types of propellants is comparable. Iodine seems to have advantages at lower mass flows whereas xenon is more power efficient at higher mass flows. Performance mappings of the RIT-10 operated with iodine show a pronounced increase of the required RFG power at high mass flows. This behavior cannot simply be related to the intensity variations of the optical emission of the different species, i.e. atomic, ionic, and molecular iodine. Additional experiments such as Langmuir measurements of the electron temperature inside the plasma, mass spectroscopy of the extracted ion beam to determine its species, and measurements of the neutral gas density in front of the thruster are required to yield additional microscopic information. Such full sets of microscopic parameters then can serve as input data for global model calculations. The combination of experimental and theoretical studies will yield a better understanding of the performance curves measured and, thus, contribute to the optimization of electric thrusters operating with iodine.

## References


[1] Tsay, M., Frongillo, J., and Hohman, Iodine-Fueled Mini RF Ion Thruster for CubeSat Applications, *34th IEPC Conference*, IEPC-2015-273, Kobe, Japan, 2015.

[2] Szabo, J., Robin, M., Paintal, S., Pote, B., Hruby, V., and Freeman, C., Iodine Propellant Space Propulsion, *33rd IEPC Conference*, IEPC-2013-311, Washington, D.C., USA, 1013.

[3] Grondein, P., Lafleur, T., Chabert, P., and Aanesland, A., "'Global model of an iodine gridded plasma thruster"', *Physics of Plasmas*, 23:3, 2016.

[4] Volkmar, C. and Ricklefs, U., "Implementation and Verification of a Hybrid Performance and Impedance Model of Gridded Radio-Frequency Ion Thrusters", *European Physical Journal D* 69(10), 227, 2015.

[5] Prince, B. D., Bemish, R. J., and Levandier, D. J, "'Application of a First Generation Collisional Radiative Model for Iodine to Optical Emissions from the Plume of an Iodine Hall Effect Thruster"', *53rd AIAA, SAE, ASEE Joint Propulsion Conference*, Atlanta, USA, 2017.